SUPPLEMENTARY INFORMATION

Supplementary Data

Supplementary Figure 1.

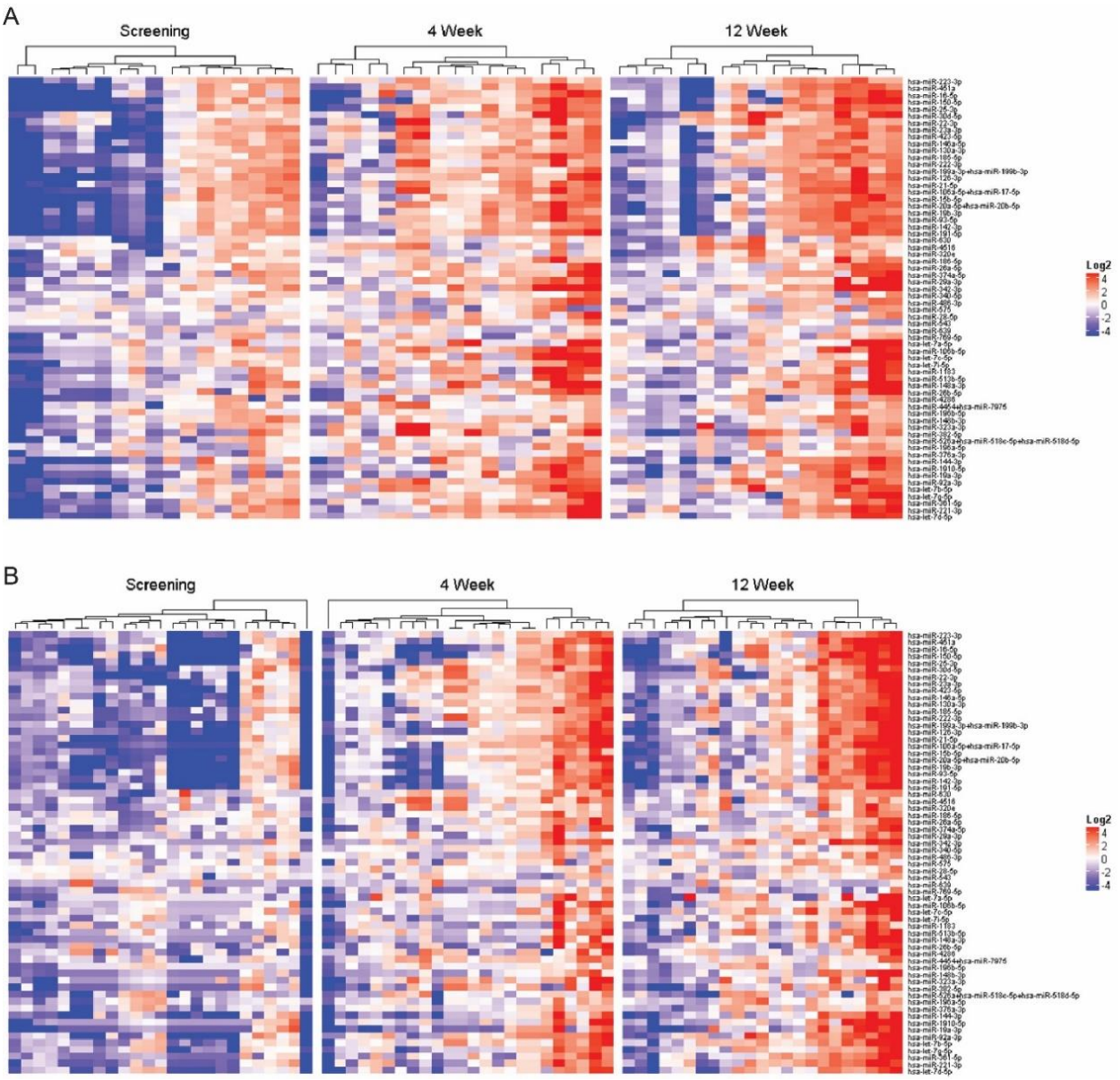

Figure S1. Fecal Microbiota Transplantation (FMT) delivered by capsule and colonoscopy to patients with recurrent *C. difficile* infection regulates the levels of circulating miRNAs. Heatmap representation of the upregulated circulating miRNAs 4 and 12 weeks after FMT treatment compared to the screening time point, as assessed by the nCounter Nanostring platform in recipients of *(A)* colonoscopy and *(B)* pill FMT.

Supplementary Figure 2.

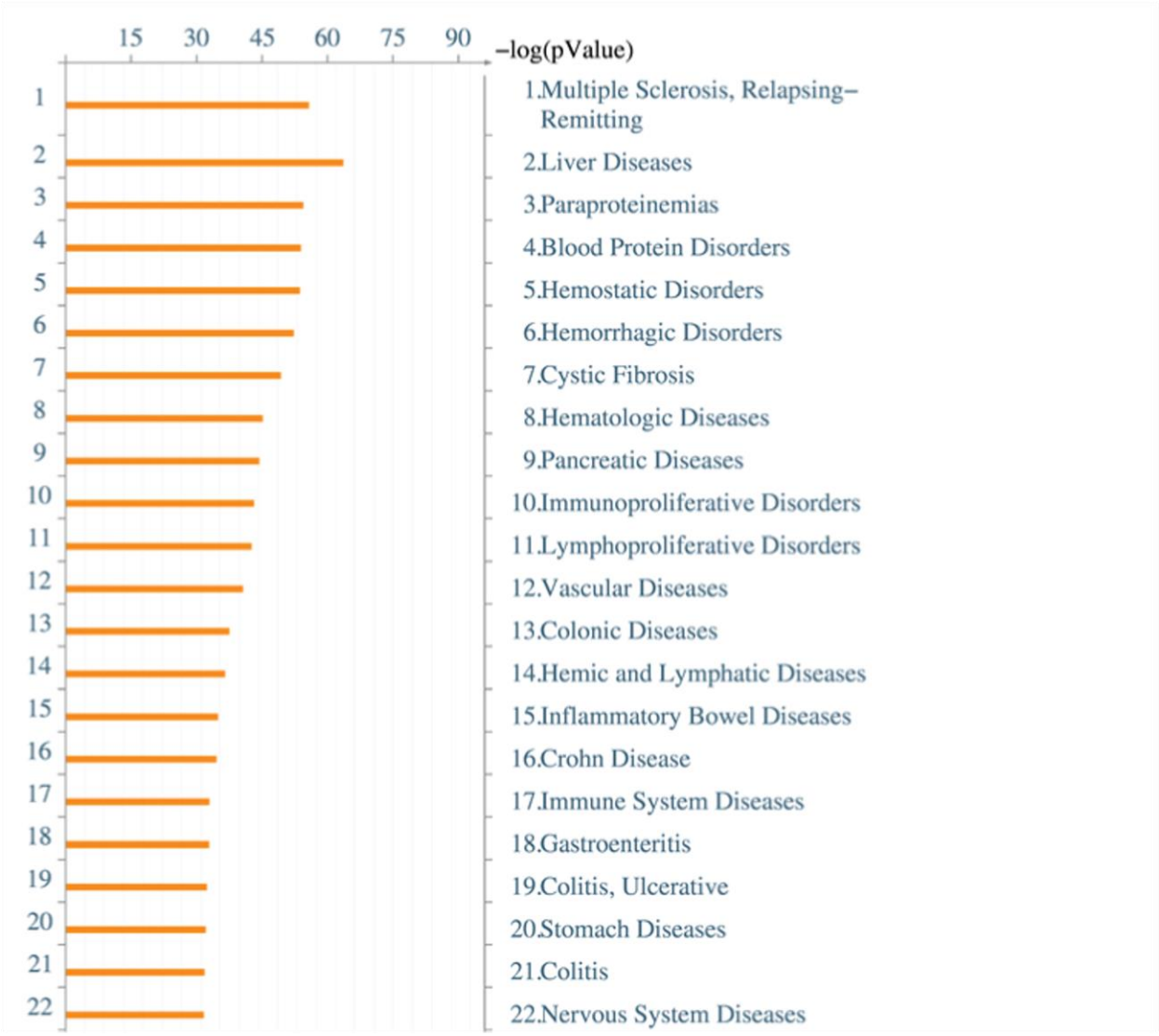

Fig S2. Circulating miRNAs changing after FMT treatment link with other pathologies. Potential applicability of FMT in other pathologies based on miRNA signatures. Analysis performed using the Metacore pathway analysis software.

Supplementary Figure 3.

Fig S3. FMT-regulated miRNAs may provide mechanistic insights into FMT therapeutic applications. Circulating miRNAs changing after FMT associate with cell/tissue properties. Analysis performed using the Metacore pathway analysis software.

Supplementary Figure 4.

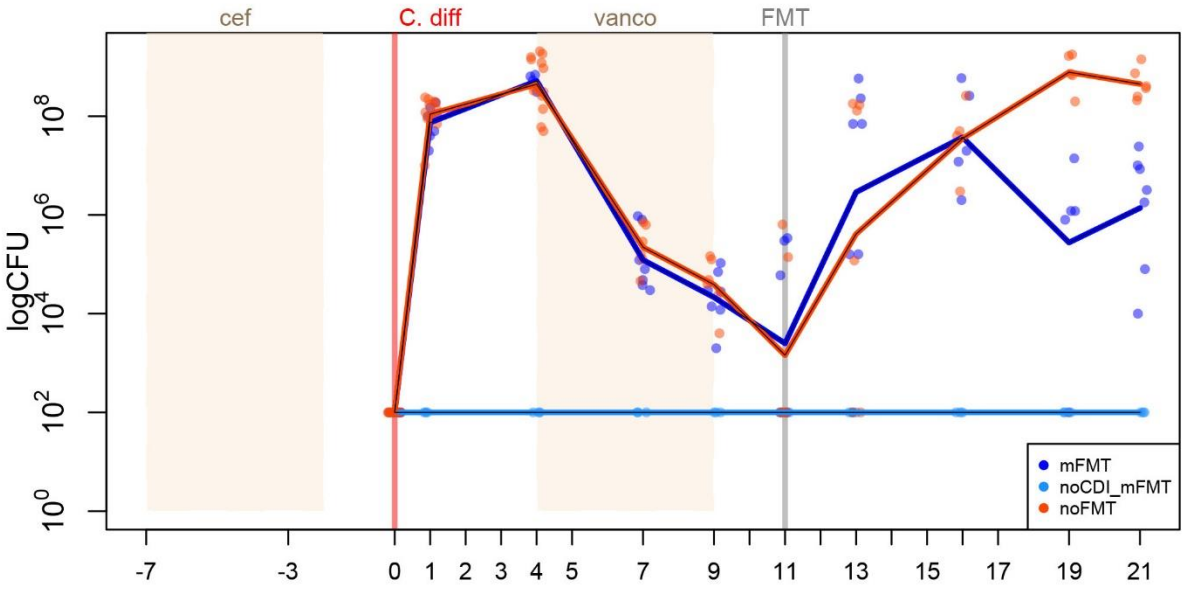

Fig S4. *C. difficile* load in animals infected with *C. difficile* strain 630 and treated with FMT. The *C. difficile* load, throughout the experiment, was assessed in individual fecal samples on taurocholate cycloserine cefoxitin fructose agar under anaerobic conditions after overnight incubation and is expressed as colony-forming unit/mL.

Supplementary Figure 5.

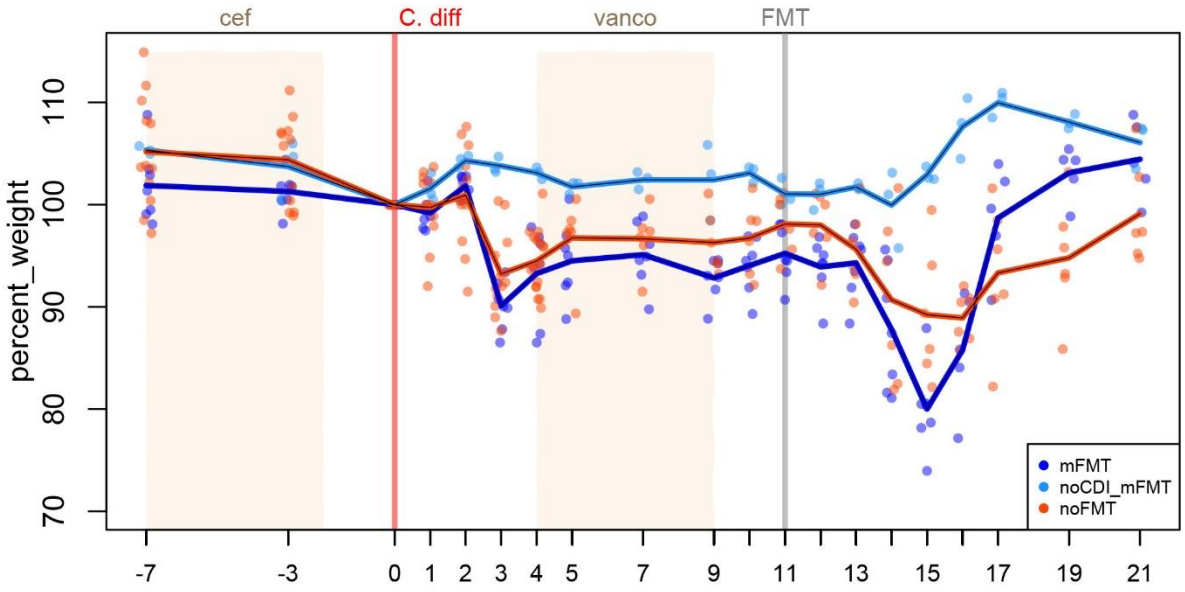

Fig S5. Body weights of animals infected with *C. difficile* strain 630 and treated with FMT. Body weight was assessed for individual animals and is expressed as % change compared to time point 0 (day of infection) per experimental group.

Supplementary Figure 6.

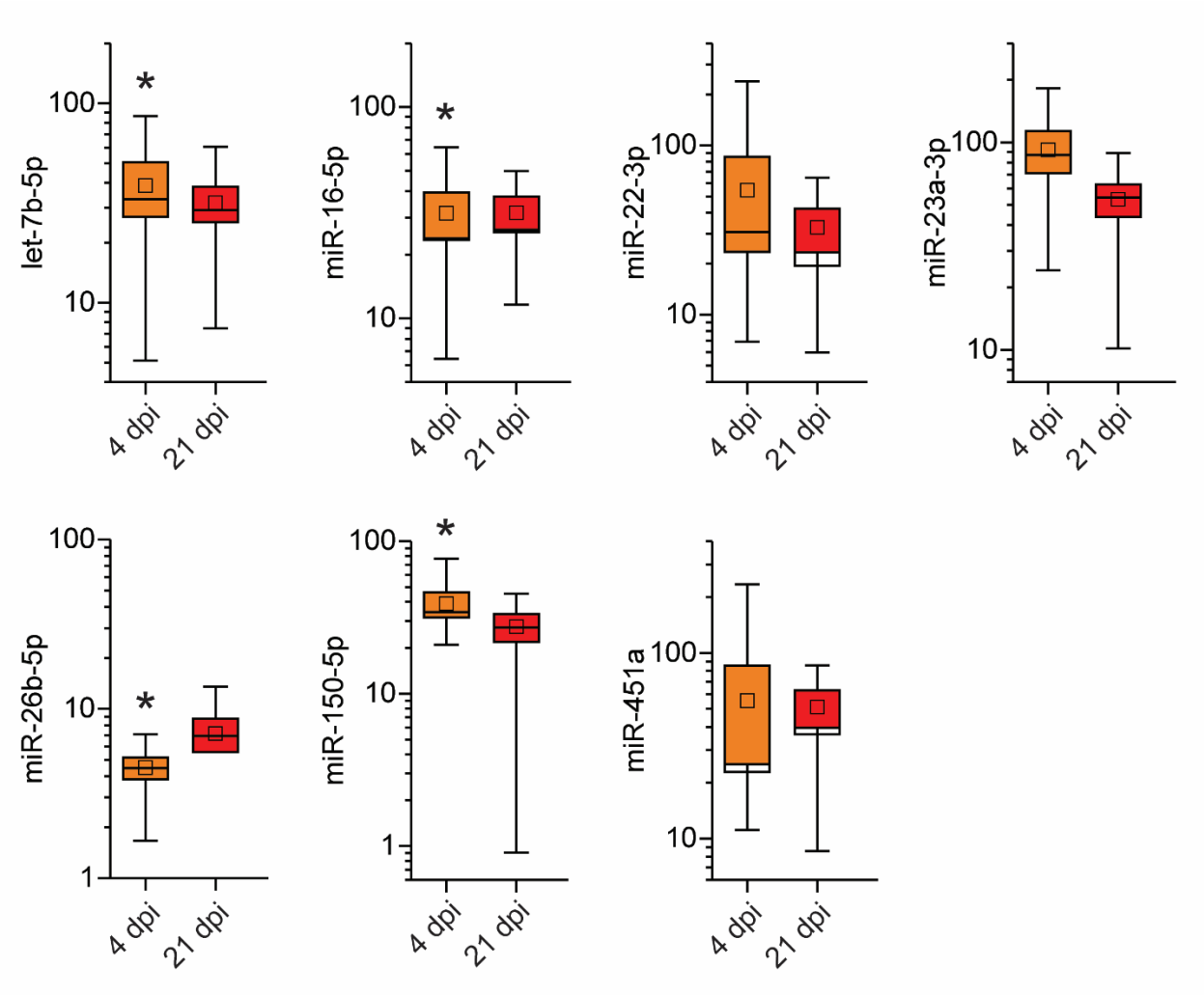

Fig S6. Effects of *C. difficile* strain 630 on circulating miRNAs in the mouse model of recurrent CDI. Box plots depicting the changes in miRNA levels in sera from mice infected with *C. difficile*, 4- and 21-days post infection (dpi). Box plots denote mean % change ± s.e.m., inner boxes represent mean, and error bars represent 95% confidence interval. miRNA levels were assessed by RT-qPCR normalized against RNU1A1 and cel-miR-39 (spike-in), and compared to control group (FMT donors), set as 100%. Statistical significance was determined by Student's *t*-test, $*P < 0.05$ (compared to donor). The 21 dpi data (statistical analysis provided in Fig. 2A) are included for comparisons.

Supplementary Figure 7.

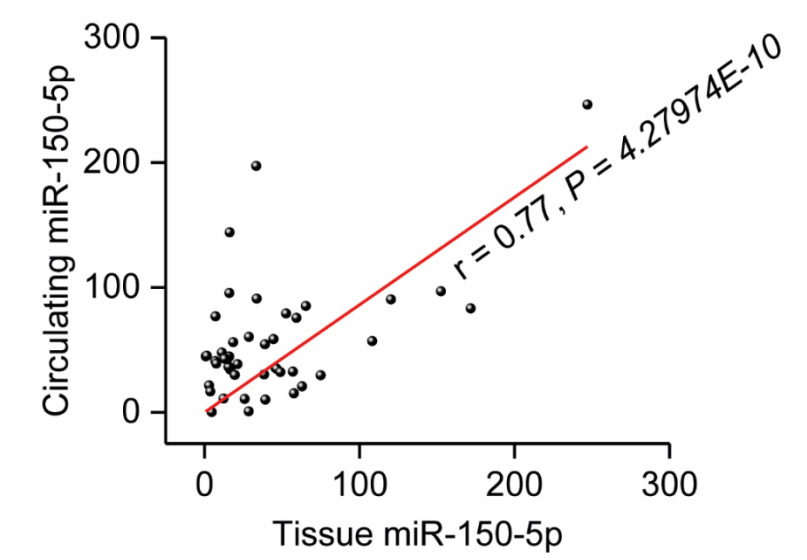

microRNA	Pearson's r	*P value*
miR-150-5p	0.77	*4.27974E-10*
miR-22-3p	0.65	*1.66563E-6*
miR-23a-3p	0.58	*3.69214E-5*
miR-451a	0.56	*6.73029E-5*
let-7b-5p	0.53	*1.74428E-4*
miR-16-5p	0.43	*0.00291*
miR-26b-5p	0.43	*0.0034*

Fig S7. Positive correlation between the levels of circulating and tissue-expressed miRNAs in the mouse model of rCDI. Correlation of miRNAs suppressed by rCDI and upregulated by FMT as assessed by Spearman's rank coefficient (and statistical significance). Upper panel, example of linear fitting for miR-150-5p levels in matched sera and ceca of individual animals.

Supplementary Figure 8.

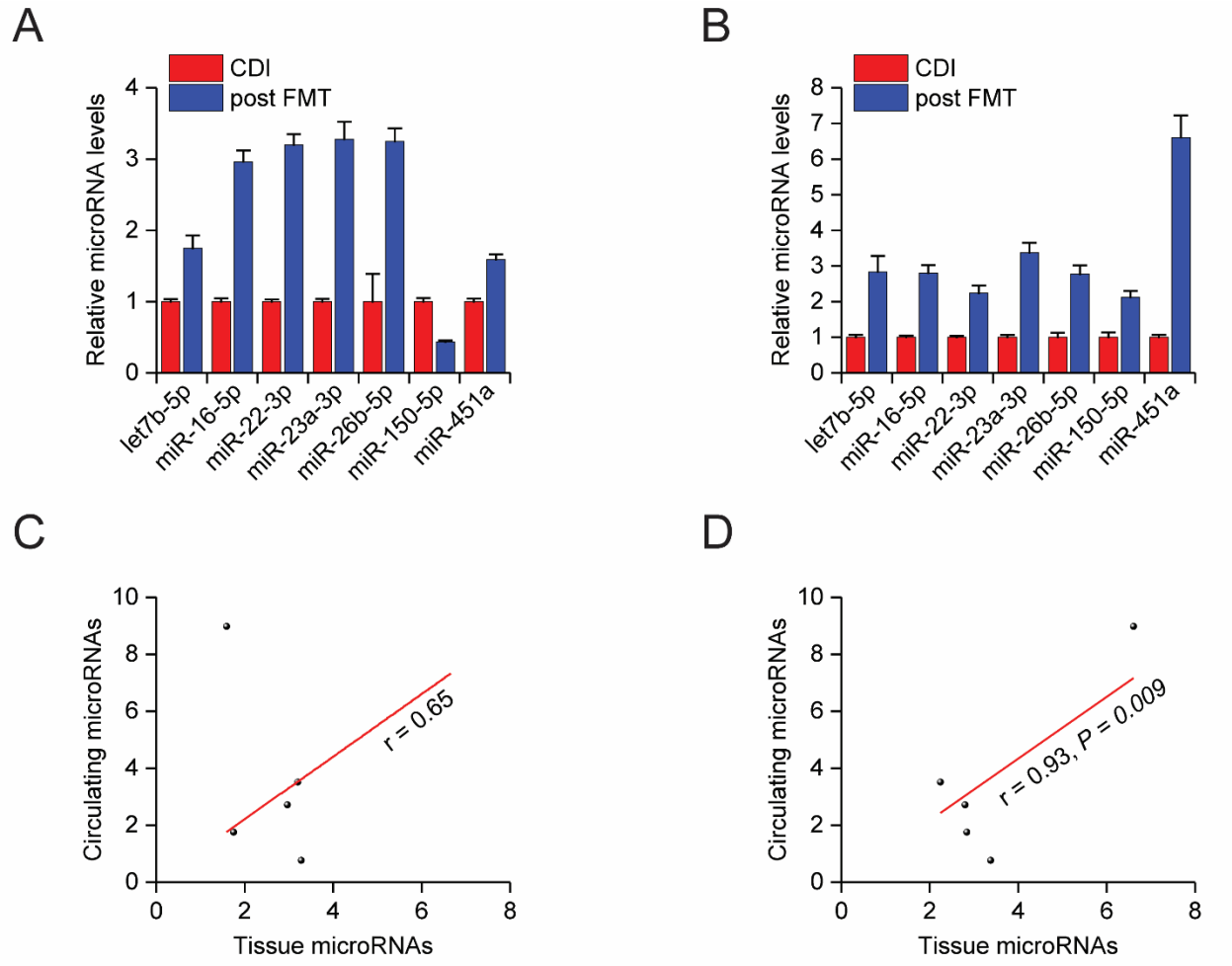

Fig S8. Positive correlation between the levels of circulating and tissue-expressed miRNAs in an 84-year old male patient with fulminant CDI pre and post FMT delivered by colonoscopy. *(A-B)* Changes in tissue miRNA levels in biopsies from *(A)* ascending and *(B)* descending colon pre and post FMT. *(C-D)* Correlation of changes in the levels of circulating miRNAs upregulated by FMT with changes in *(C)* ascending and *(D)* descending colonic tissue-expressed miRNAs in the same patient. MicroRNA levels were assessed by RT-qPCR and normalized against RNU1A1 and 5S rRNA for tissues and RNU1A1 and cel-miR-39 (spike-in) for sera and are expressed as mean ± s.e.m. compared to control samples, set as 1. Correlations were assessed by Spearman's rank coefficient.

Supplementary Figure 9.

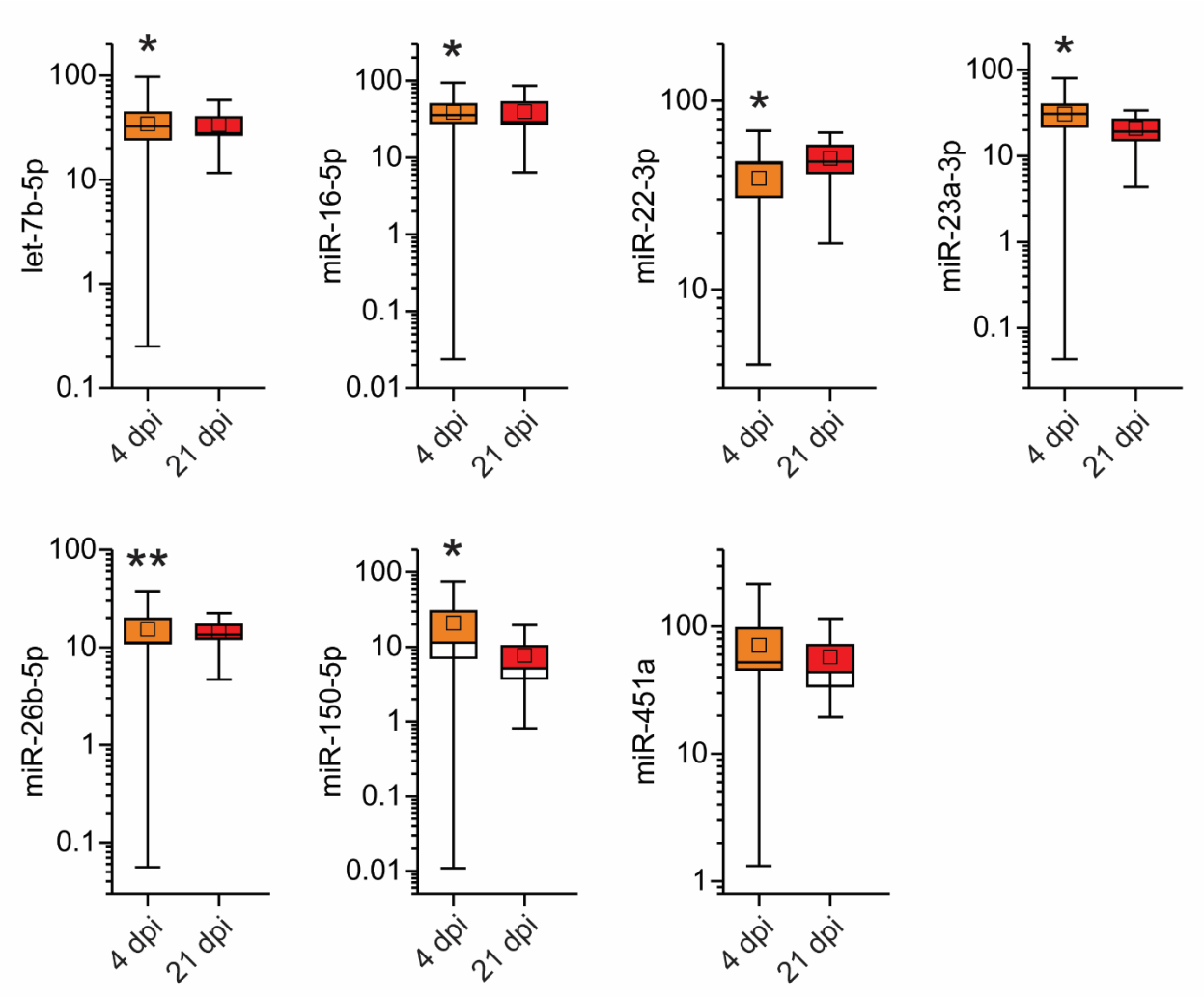

Fig S9. Effects of *C. difficile* strain 630 on intestinal tissue miRNAs in a mouse model of recurrent CDI. Box plots depicting the changes in miRNA levels in ceca from mice infected with *C. difficile*, 4- and 21-days post infection (dpi). Box plots denote mean % change ± s.e.m., inner boxes represent mean, and error bars represent 95% confidence interval. miRNA levels were assessed by RT-qPCR normalized against RNU5G and 5S rRNA, and compared to control group (FMT donors), set as 100%. Statistical significance was determined by Student's *t*-test, $*P < 0.05$, $**P < 0.01$ (compared to donor). The 21 dpi data (statistical analysis provided in Fig. 2B) are included for comparisons.

Supplementary Figure 10.

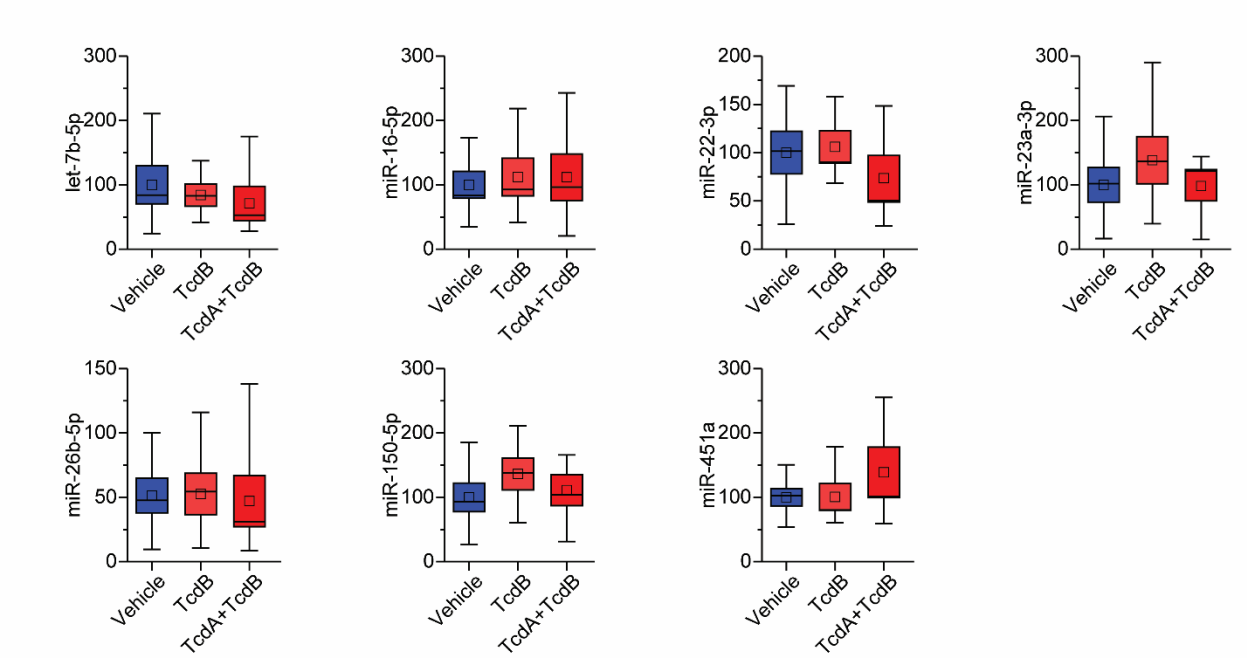

Fig S10. Circulating miRNAs in mice treated by intrarectal instillation with *C. difficile* whole toxins (derived from VPI 10463 reference strain). Box plots depicting the changes in miRNA levels in sera from animals treated with TcdB, combination of TcdA with TcdB, compared to HBSS-treated controls (Vehicle). Box plots denote mean % change ± s.e.m., inner boxes represent mean, and error bars represent 95% confidence interval. miRNA levels were assessed by RT-qPCR and were normalized against RNU1A1 and cel-miR-39, and compared to control samples, set as 100%.

Supplementary Figure 11.

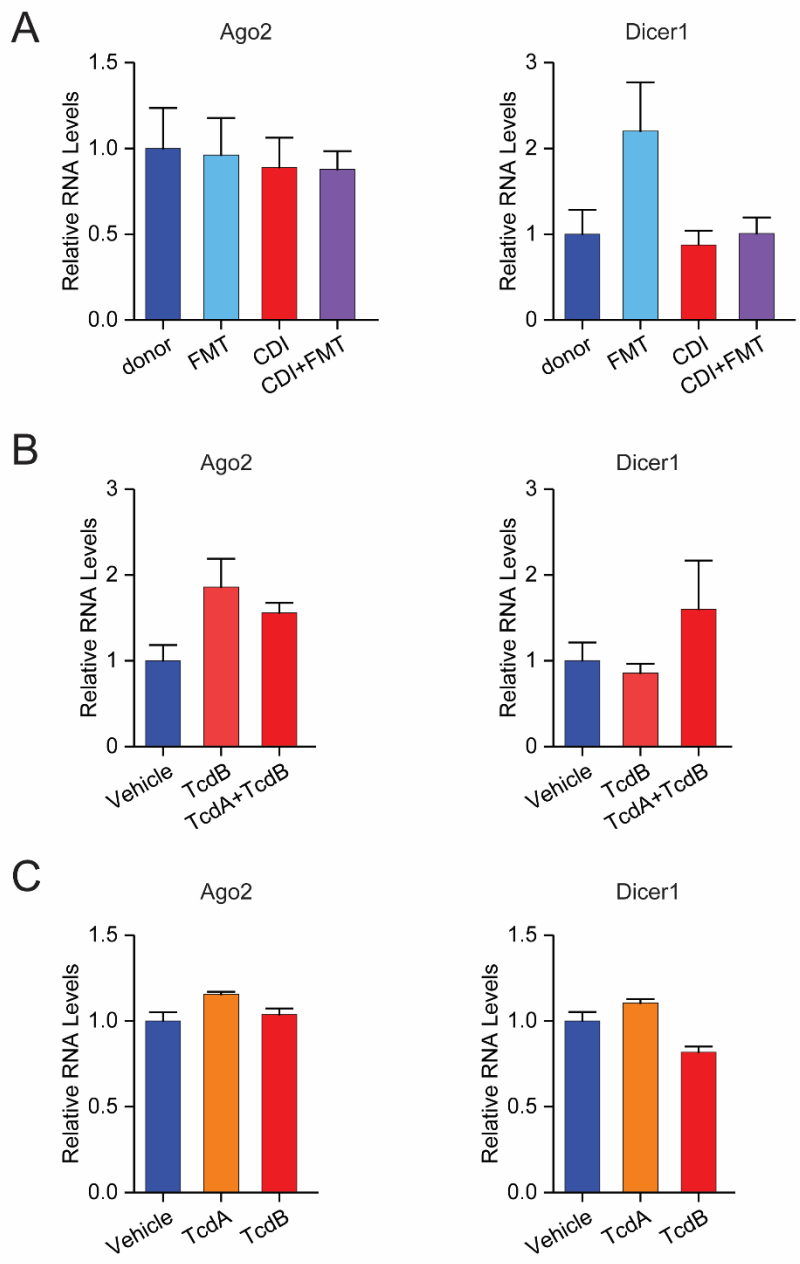

Fig S11. Effects of *C. difficile* infection on Ago2 and Dicer1 expression. Ago2 and Dicer1 mRNA levels in *(A)* ceca from animals treated with FMT, infected with *C. difficile* (CDI), and infected with *C. difficile* and treated with FMT (CDI+FMT), compared to FMT donors, *(B)* colonic tissues from animals treated with TcdB or combination of TcdA with TcdB, compared to controls (Vehicle), *(C)* colonoids treated with TcdA or TcdB, compared to DMEM-treated controls (Vehicle). mRNA levels assessed by RT-qPCR were normalized against beta-Actin and GAPDH and are expressed as mean± s.e.m. compared to control samples, set as 1.

Supplementary Figure 12.

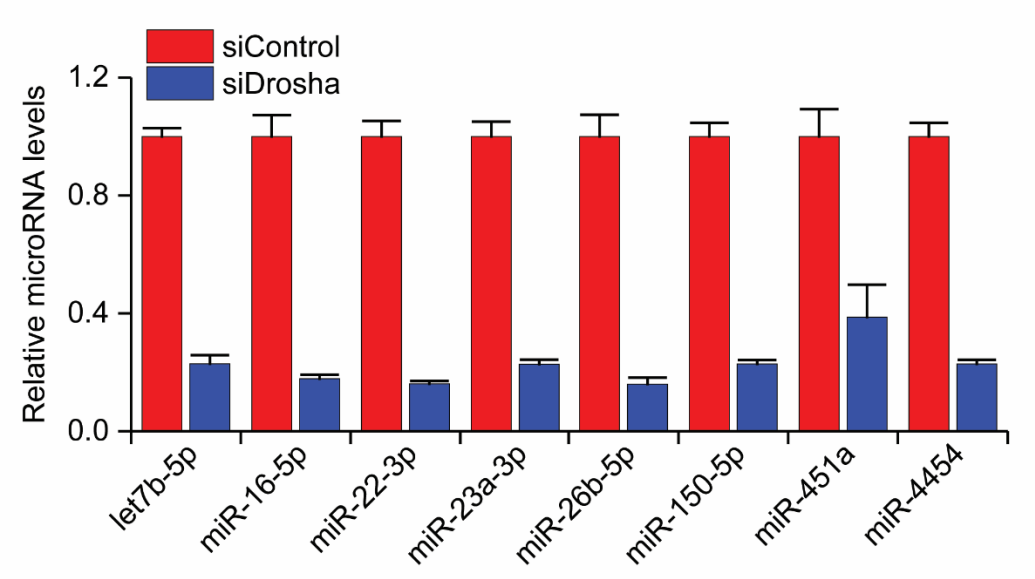

Fig S12. miRNA levels in NCM356 cells upon knockdown of Drosha. Drosha was knocked down by means of siRNA (5nM) and 48h later miRNA levels were assessed by RT-qPCR. Data expressed as mean ± s.e.m. compared to control non-targeting siRNA (siControl) transfected cells, set as 1.

Supplementary Figure 13.

	Circulating Proteins			
Circulating microRNAs	**IL12B**	**IL18**	**FGF21**	**TNFRSF9**
miR-23a-3p	**-0.220 (0.032)**		-0.284 (0.005)	
miR-150-5p		**-0.226 (0.028)**		
miR-26b-5p			**-0.305 (0.003)**	
miR-130a-3p			-0.257 (0.012)	
miR-20a-5p+miR 20b-5p				-0.205 (0.046)
miR-28-5p				**-0.238 (0.020)**

Fig S13. Inverse correlation between the circulating levels of miRNAs and protein levels of their predicted targets. Correlation of miRNAs upregulated by FMT with predicted target cytokines/chemokines as assessed by Spearman's rank coefficient (and statistical significance). Highlighted in red the interactions validated experimentally by RT-qPCR and 3'UTR activity reporter assays, after miRNA overexpression in colonic epithelial cells (Figure 5).

Supplementary Figure 14.

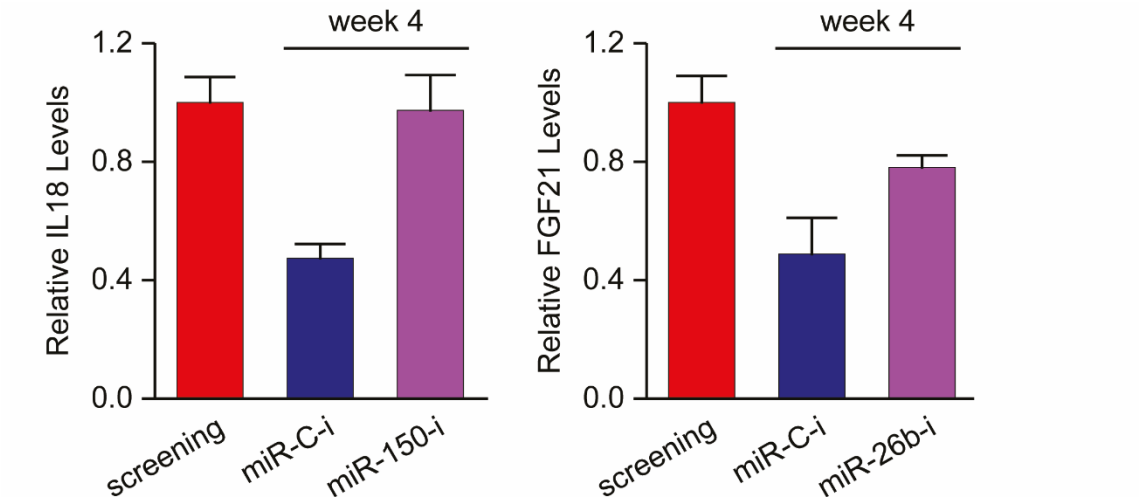

Fig S14. Functional effects of Fecal Microbiota Transplantation (FMT)-regulated circulating miRNAs in patients with *C. difficile* infection. PBMCs derived from a patient 4 weeks post FMT were treated with miRNA inhibitors and analyzed for the levels of their respective targets 24 hours later. The RNA levels of IL18 and FGF21 were assessed by RT-qPCR, normalized against beta-Actin and GAPDH levels and are expressed as mean ± s.e.m. compared to PBMCs collected at screening (pre-FMT), set as 1. miR-C-i, a non-targeting miRNA inhibitor, was used as control.

Supplementary Figure 15.

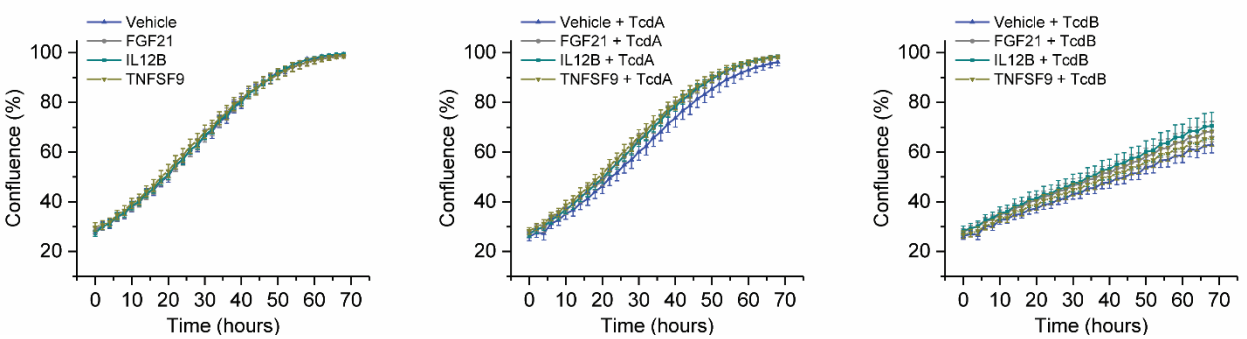

Fig S15. Effects of cytokines regulated by FMT in combination with *C. difficile* exotoxins (VPI 10463 reference strain) on epithelial cell growth. NCM356 cells pretreated with FGF21, IL12B and TNFSF9 (50ng/ml) or Vehicle where exposed to 10pM TcdA (middle panel) or TcdB (right panel) and cell growth was monitored in real time and expressed as % of confluence (IncuCyte).

Supplementary Figure 16.

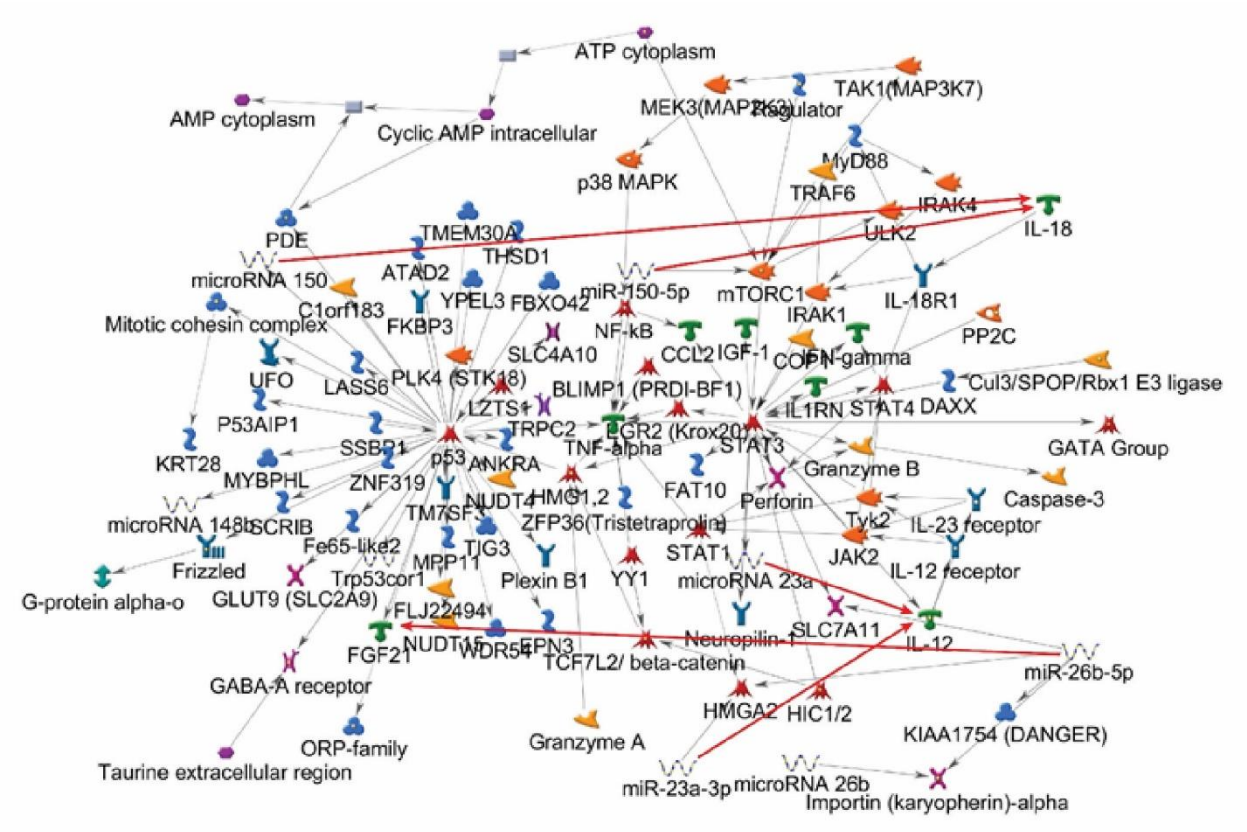

Fig S16. The effects of miR-23a, miR-150 and miR-26b on IL12B, IL18 and FGF21, respectively, provide novel links between metabolic and inflammatory networks. The miRNA-regulated pathways with the new links (red arrows), assessed using the Metacore network analysis software.

Supplementary Figure 17.

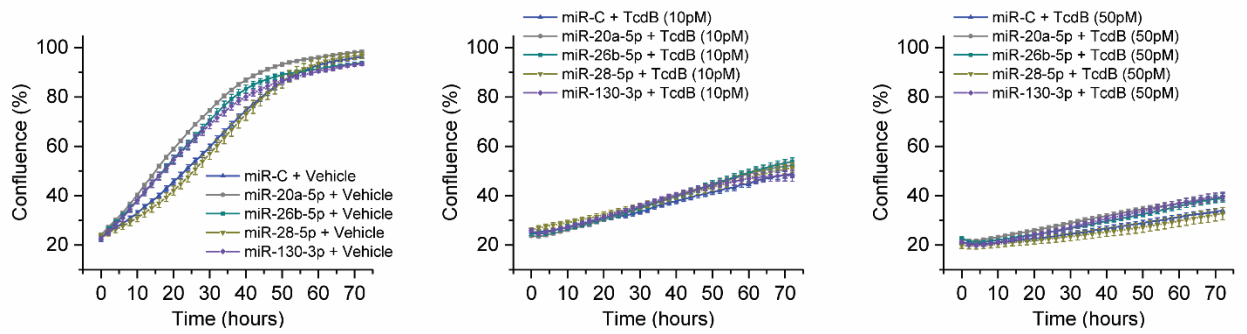

Fig S17. Effects of microRNAs regulated by FMT in combination with TcdB on epithelial cell growth. NCM356 cells transfected with miR-20a-5p, miR-26b-5p, miR-28-5p, miR-130a-3p or miR-C, where exposed to 10pM (middle panel) or 50pM (right panel) of TcdB or Vehicle (left panel) and cell growth was monitored in real time and expressed as % of confluence (IncuCyte). miR-C (cel-miR-39-3p), a non-targeting miRNA, was used as negative control.

Supplementary Figure 18.

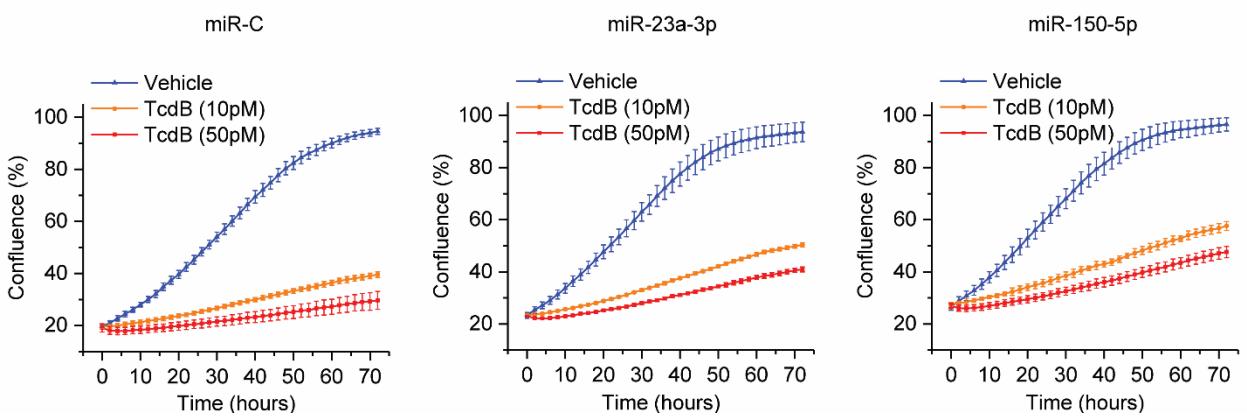

Fig S18. Effects of microRNAs regulated by FMT in combination with TcdB on epithelial cell growth. NCM356 cells transfected with miR-23a-3p, miR-150-5p or miR-C, where exposed to TcdB or Vehicle (left panel) and cell growth was monitored in real time and expressed as % of confluence (IncuCyte). miR-C (cel-miR-39-3p), a non-targeting miRNA, was used as negative control.

Supplementary Figure 19.

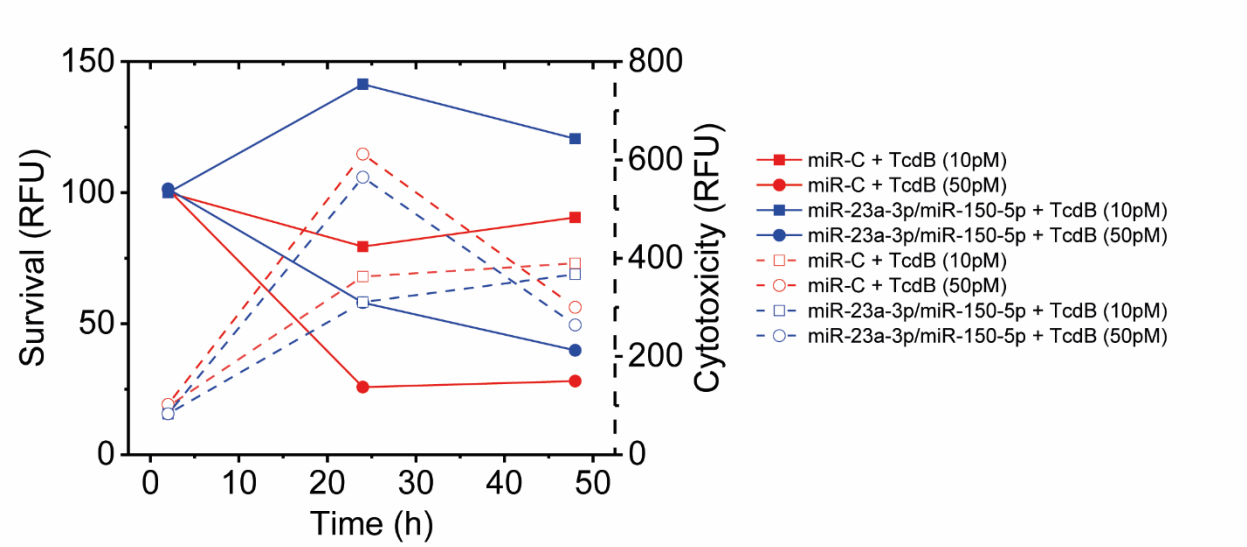

Fig S19. Effects of microRNAs regulated by FMT on TcdB-induced cytotoxicity and cell survival. NCM356 cells transfected with miR-23a-3p and miR-150-5p or miR-C, where exposed to TcdB and cytotoxicity and survival was monitored using the Apotox Glo assay. Results are expressed as % survival (solid lines) or ratio of cytotoxicity against surviving cells (dotted lines). miR-C (cel-miR-39-3p), a non-targeting miRNA, was used as negative control.

Supplementary Figure 20.

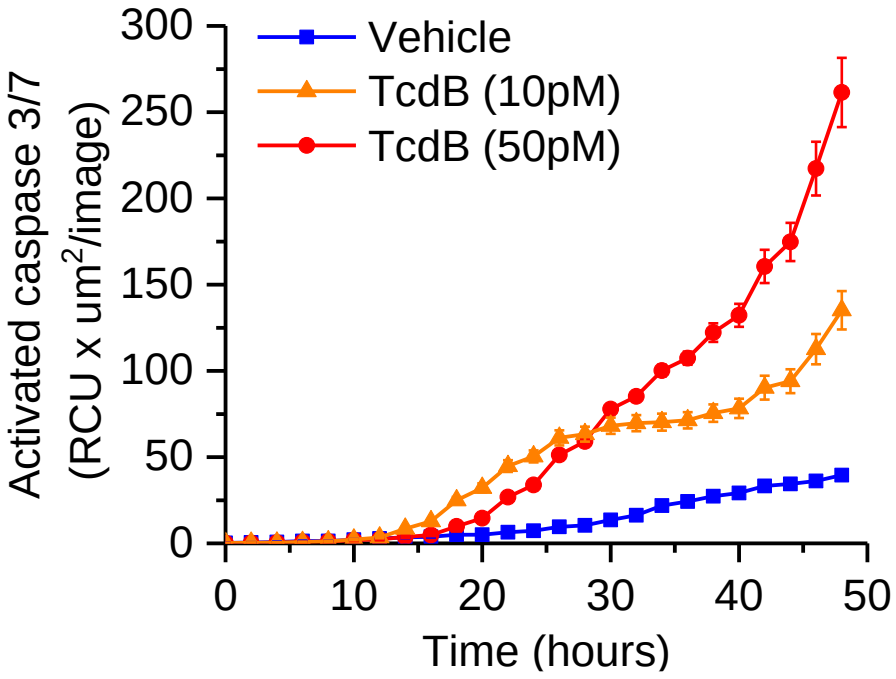

Fig S20. Effects of TcdB on cell apoptosis. NCM356 where exposed to TcdB and apoptosis was monitored in real-time as activated caspase3/7 fluorescence (IncuCyte).

Supplementary Figure 21.

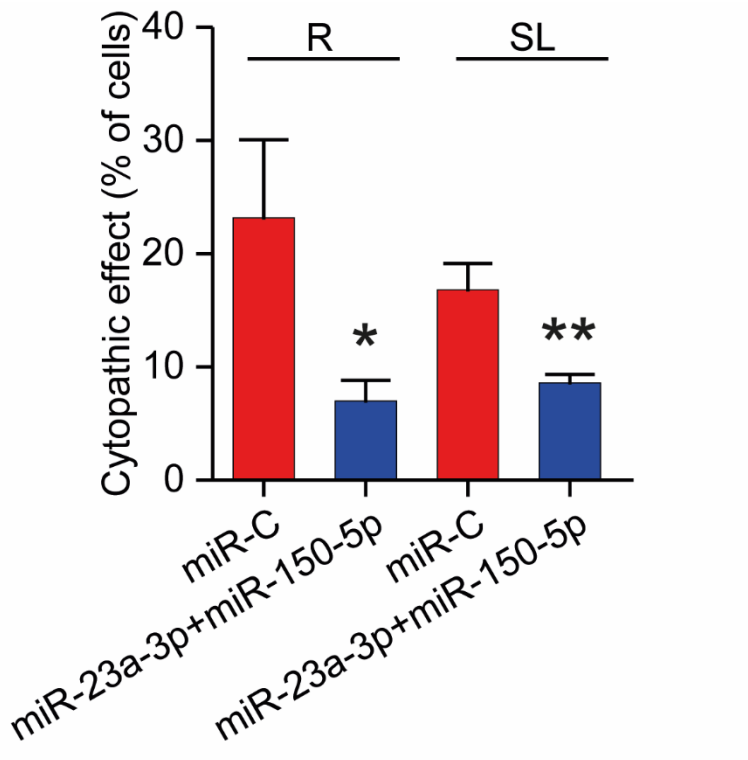

Fig S21. Effects of miR-23a-3p and miR-150-5p overexpression on TcdB-mediated cytoskeleton rearrangements. NCM356 cytoskeleton organization was studied by fluorescence microscopy after phalloidin staining. Cells were scored by two independent researchers blind to the treatments and the ratio of morphologically altered cells were expressed as % of the total number of cells per field. miR-C (cel-miR-39-3p), a non-targeting miRNA, was used as negative control. Statistical significance was determined by Student's t-test, *P < 0.05, **P < 0.01. R, rounded cells; SL, spindle like cells.